

SCIENTIFIC PAPERS
OF THE UNIVERSITY OF PARDUBICE
Series A
Faculty of Chemical Technology
16 (2010)

**OPTICAL PROPERTIES OF Tl-DOPED Bi_2Se_3
SINGLE CRYSTALS**

Petr JANÍČEK^a, Čestmír DRAŠAR^{a1}, Anna KREJČOVÁ^b, Petr LOŠŤÁK^c
and Jiří NAVRÁTIL^d

^aInstitute of Applied Physics and Mathematics,

^bInstitute of Environmental and Chemical Engineering,

^cDepartment of Inorganic Chemistry,

^dJoint Laboratory of Solid State Chemistry,
The University of Pardubice, CZ–532 10 Pardubice,

Received September 29, 2010

$\text{Bi}_{2-x}\text{Tl}_x\text{Se}_3$ single crystals with the Tl content of $c_{\text{Tl}} = 0$ to 5.2×10^{24} atoms m^{-3} prepared from the elements of 5N purity by means of a modified Bridgman method were characterized by the measurements of infrared reflectance and transmittance. The values of the plasma resonance frequency ω_p , optical relaxation time τ , and high-frequency permittivity ϵ_∞ were determined by fitting the reflectance spectra using plasma-resonance formula. It was found that the substitution of Tl atoms for Bi atoms in the Bi_2Se_3 crystal lattice leads to a decrease in the ω_p values implying a decrease in the free carrier concentration. This effect is explained within a model of the point defects in the crystal lattice of $\text{Bi}_{2-x}\text{Tl}_x\text{Se}_3$. The dependences of the absorption coefficient K on the energy of incident photons were determined from the transmittance spectra. The optical

¹ To whom correspondence should be addressed.

width of the energy gap decreases with the increasing Tl content. The values of the exponent β from the relation of $K \sim \lambda^\beta$ for the long-wavelength absorption edge range within the interval from 2.1 to 2.5 indicating the dominant scattering mechanism of free current carriers is the scattering on acoustic phonons.

Introduction

Bismuth selenide Bi_2Se_3 belongs to the family of narrow-band semiconductors $\text{A}_2^{\text{V}}\text{B}_3^{\text{VI}}$ (where A = Bi, Sb and B = Se, Te) with tetradymite structure (space group $D_{3d}^5 - R\bar{3}m$). It is the component of the solid solution, for example $\text{Bi}_2\text{Te}_{3-x}\text{Se}_x$ and $\text{Bi}_{2-x}\text{Sb}_x\text{Te}_{3-y}\text{Se}_y$, that form the base materials for *n*-type room temperature thermoelectric (TE) devices having dimensionless figure of merit $ZT = \sigma S^2 T / \kappa$ (σ , S , κ and T stand for electrical conductivity, Seebeck coefficient, thermal conductivity, and temperature, respectively) value close to 1 [1]. Since the physical quantities are dependent on free carrier concentration, the influence of dopants on the free carrier concentration is one of active research areas. Despite considerable research on this material [2], there is a couple of papers on the influence of IIIB elements (Ga, In, Tl) on the properties of Bi_2Se_3 single crystals. There are a few papers concerning the doping with Ga [3] and In [4,5] and its influence on the optical properties of Bi_2Se_3 . While Ga increases the concentration of free electrons N , In increases N just at low indium content whereas In leads to a decrease of N at higher concentrations. The effect of thallium doping was studied only in our previous paper [6], where the results of measurement of the transport coefficients (Hall coefficient, electrical conductivity and Seebeck coefficient) were published. Tl doping results in a decrease of the free electron concentration as well as in an increase of mobility of the free electrons in Bi_2Se_3 matrix. The effect of Tl doping on the optical properties of Bi_2Se_3 single crystals has not been studied yet.

The aim of this paper is to describe the preparation of the single crystals $\text{Bi}_{2-x}\text{Tl}_x\text{Se}_3$ for $x = 0-0.1$ and their characterization by the measurement of the reflectance in the plasma-resonance frequency region and the transmittance in infrared region. The observations are explained in terms of the point-defect model, which is based on the idea that the Tl impurities create substitutional defects and influence the concentration of native defects in Bi_2Se_3 as well.

Experimental

The single crystals of $\text{Bi}_{2-x}\text{Tl}_x\text{Se}_3$ with nominal x values between 0 and 0.1 have been grown using the Bridgman method. The polycrystalline precursor was synthesized by heating of stoichiometric mixtures of 99.999 % pure Bi, Se and

TlSe. The synthesis of TlSe was carried out by heating stoichiometric mixtures of 5N purity Se and Tl at the temperature of 800 K for 1 hour in evacuated quartz ampoules. This material was powdered and combined with Bi and Se in the ratio corresponding to the stoichiometry $\text{Bi}_{2-x}\text{Tl}_x\text{Se}_3$ ($x = 0, 0.01, 0.02, 0.06$ and 0.10) and synthesis of the polycrystalline product was carried out in evacuated conical quartz ampoules in a horizontal furnace at the temperature of 1200 K for 48 hours. Then the samples were annealed at the temperature of 1100 K for 24 hours in the vertical Bridgman furnace and lowered into the zone with the temperature gradient of 125 K cm^{-1} with the rate of 1.3 mm h^{-1} .

The obtained crystals were 60 mm long with 8 mm diameter and could be easily cleaved. Their trigonal axis c was always perpendicular to the pulling direction so that the (0001) plane was parallel to the ampoule axis. The orientation of the single crystal was carried out using the Laue back-diffraction technique which confirmed that the planes were always (0001).

Samples for the reflectance and transmittance measurements were cut out from the central part of the crystals. Thin samples (with the thickness of several μm) for the transmittance measurements were obtained using an adhesive tape for cleaving thin layers from the crystal.

Spectral dependences of the reflectance R in the plasma resonance frequency range were measured at room temperature in unpolarized light on natural (0001) cleavage faces using an FT-IR spectrometer Bruker IFS 55. The geometry of the experiment was such that the electric field vector \vec{E} of the electromagnetic radiation was always perpendicular to the trigonal c -axis, i.e. $\vec{E} \perp c$.

The measurements of the transmittance spectra on thin samples were carried out at room temperature using the same spectrometer. The radiation was unpolarized, but the orientation of the samples with respect to the incident radiation always fulfilled the condition $\vec{E} \perp c$.

The actual concentration of thallium (c_{Tl}) in the samples for measurements of reflectance and transmittance was determined using the atomic emission spectrometry (AES).

Results and Discussion

Reflectance Spectra

The reflectance spectra are depicted in Fig. 1. For lucidity the curves of the doped samples are shifted by the constant values 0.3, 0.6, 0.9 and 1.2 for $\text{Bi}_{1.99}\text{Tl}_{0.01}\text{Se}_3$, $\text{Bi}_{1.98}\text{Tl}_{0.02}\text{Se}_3$, $\text{Bi}_{1.94}\text{Tl}_{0.06}\text{Se}_3$, and $\text{Bi}_{1.9}\text{Tl}_{0.1}\text{Se}_3$, respectively. It is evident that the reflectance curves $R = f(\bar{\nu})$ reveal distinct minima which confirm a good single crystal quality. The positions of the minima $\bar{\nu}_{\text{min}}$ are given in Table I. One can see

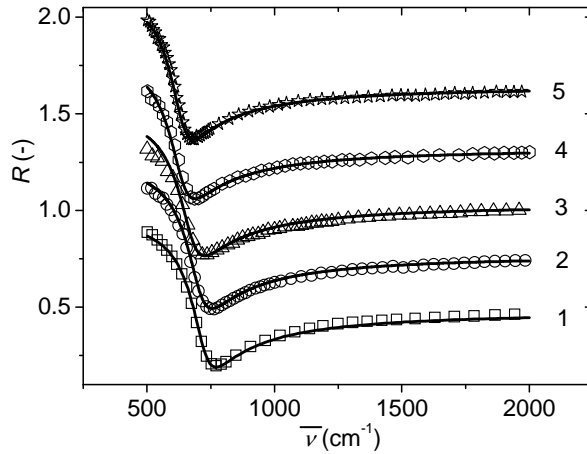


Fig. 1 Reflectance spectra of $\text{Bi}_{2-x}\text{Tl}_x\text{Se}_3$ single crystals (samples are labeled according to Table I). Symbols represent the experiment; the solid lines are fits according to plasma-resonance formula

Table I Optical parameters of $\text{Bi}_{2-x}\text{Tl}_x\text{Se}_3$ single crystals

Sample No.	Nominal composition	c_{Tl} (AES) 10^{24} m^{-3}	Actual x	$\bar{\nu}_{\text{min}}$	ϵ_{∞}
1	Bi_2Se_3	0	0	771	29.0
2	$\text{Bi}_{1.99}\text{Tl}_{0.01}\text{Se}_3$	0.2	3.2×10^{-5}	752	29.5
3	$\text{Bi}_{1.98}\text{Tl}_{0.02}\text{Se}_3$	1.1	1.6×10^{-4}	734	28.0
4	$\text{Bi}_{1.94}\text{Tl}_{0.06}\text{Se}_3$	4.4	6.41×10^{-4}	696	26.5
5	$\text{Bi}_{1.9}\text{Tl}_{0.1}\text{Se}_3$	5.2	7.69×10^{-4}	677	25.5
		ω_p 10^{14} s^{-1}	τ 10^{-14} s	N/m_{\perp} 10^{26} m^{-3}	K_{min} cm^{-1}
1	Bi_2Se_3	1.373	4.75	1.72	913
2	$\text{Bi}_{1.99}\text{Tl}_{0.01}\text{Se}_3$	1.340	4.50	1.67	886
3	$\text{Bi}_{1.98}\text{Tl}_{0.02}\text{Se}_3$	1.285	4.40	1.45	770
4	$\text{Bi}_{1.94}\text{Tl}_{0.06}\text{Se}_3$	1.215	4.50	1.23	653
5	$\text{Bi}_{1.9}\text{Tl}_{0.1}\text{Se}_3$	1.210	4.95	1.17	621

the shift of the minima to lower wave numbers, e.g. higher wavelength with increasing Tl content.

In order to obtain information on the changes in the free carrier concentration, associated with the incorporation of Tl into Bi_2Se_3 lattice, the experimental $R = f(\bar{\nu})$ curves were fitted using equations for the real (ϵ_1) and the imaginary (ϵ_2) parts of the complex dielectric function [7]

$$\varepsilon_1 = n^2 - k^2 = \varepsilon_\infty \left(1 - \frac{1}{\left(\frac{\omega}{\omega_p}\right)^2 + \left(\frac{1}{\omega_p \tau}\right)^2} \right) \quad (1)$$

$$\varepsilon_2 = 2nk = \frac{\varepsilon_\infty}{\omega \tau} \frac{1}{\left(\frac{\omega}{\omega_p}\right)^2 + \left(\frac{1}{\omega_p \tau}\right)^2} \quad (2)$$

where n is the index of refraction, k index of extinction, τ optical relaxation time, ε_∞ the high-frequency permittivity, and ω_p the plasma resonance frequency. For one type of carriers, the last quantity is given by the relation

$$\omega_p = \left(\frac{Ne^2}{\varepsilon_0 \varepsilon_\infty m_\perp m_0} \right)^{\frac{1}{2}} \quad (3)$$

where $m_\perp m_0$ is the free carrier effective mass in the direction perpendicular to the trigonal axis c , N is the concentration of free carriers, and ε_0 is the permittivity of the free space.

It is necessary to mention that relation (3) is not consistent with the conclusion of paper [8] obtained from the Shubnikov de Haas effect measurements at the temperature of liquid He, showing the splitting of conduction band of Bi_2Se_3 into subbands ($\Delta E \sim 40$ meV). However our measurements performed at room temperature cannot determine the influence of the conduction band splitting because the value ΔE is comparable with the energy kT .

Approximate trial values of ε_∞ , τ and ω_p were inserted in Eqs (1) and (2), and a suitable computer program was used to minimize the function

$$\sum_{n=1}^m (R'_n - R_n)^2 \quad (4)$$

where R' is the experimental reflectance and R is the calculated value, given by the relation

$$R = \frac{(n-1)^2 + k^2}{(n+1)^2 + k^2} \quad (5)$$

In Fig. 1 experimental values of reflectance R' are represented by points, theoretical dependence R acquired by the best fit of experimental values is

represented by lines. This procedure gives nice fits to the experimental results, as can be seen from Fig. 1. The values of N/m_{\perp} were calculated from ω_p using Eq. (3).

From Table I it is evident that the values of N/m_{\perp} decrease with increasing Tl content in the crystals (provided that m_{\perp} is constant it applies also for N). Incorporation of Tl atoms into the Bi_2Se_3 matrix results in the suppression of the free electron concentration. The conclusion presented above on the change of the free carrier concentration caused by Tl atoms entering the Bi_2Se_3 lattice is supported by the results of the measurements of the transport parameters presented in our previous paper [6]. We observed that with the increasing content of Tl atoms in the $\text{Bi}_{2-x}\text{Tl}_x\text{Se}_3$ samples the absolute values of Hall coefficient $R_H(\vec{B}\parallel c)$ and Seebeck coefficient $S(\Delta T_{\perp}c)$ increase.

Transmittance Spectra — Absorption Coefficient

As an illustration of the transmittance measurements, the $T = f(\bar{\nu})$ plots are presented for two samples with the highest content of Tl in Fig. 2 and 3. Well-developed interferences and a relatively high transmittance indicate a good optical quality of the prepared samples.

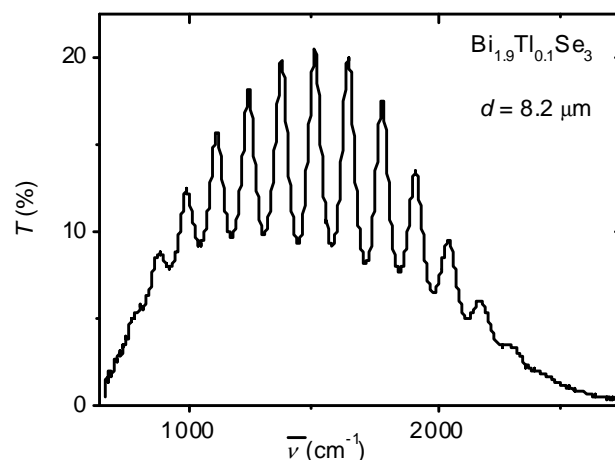


Fig. 2 Transmittance spectra of $\text{Bi}_{1.9}\text{Tl}_{0.1}\text{Se}_3$ single crystal

To determine the absorption coefficient K as a function of the incident photon energy the transmittance T and reflectance R values corresponding to the locations of the interference maxima in the $T = f(\bar{\nu})$ plot were used in the formula

$$K = \frac{1}{d} \ln \left\{ \frac{1}{T} \left[RT + \frac{1}{2}(1 - R)^2 + \frac{1}{2} \sqrt{4RT(1 - R)^2 + (1 - R)^4} \right] \right\} \quad (6)$$

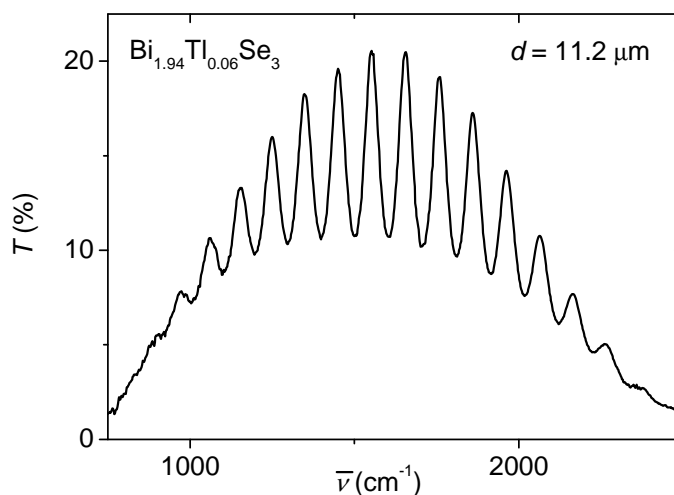


Fig. 3 Transmittance spectra of $\text{Bi}_{1.94}\text{Tl}_{0.06}\text{Se}_3$ single crystal

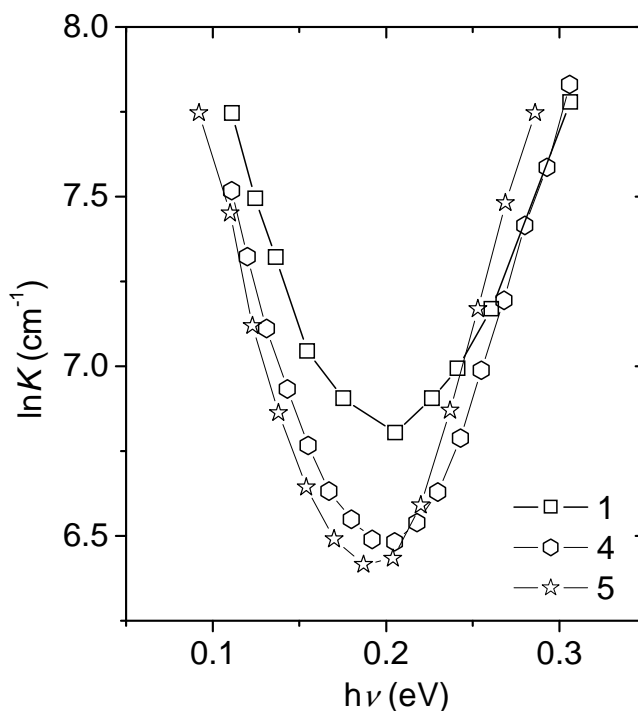


Fig. 4 Spectral dependences of absorption coefficient K of $\text{Bi}_{2-x}\text{Tl}_x\text{Se}_3$ single crystals (samples are labeled according to Table I)

where d is the sample thickness. For lucidity the results are shown only for $x = 0, 0.06$ and 0.1 in Fig. 4. Values of K for samples with $x = 0.01$ and 0.02 are very close to pure Bi_2Se_3 .

A decrease in the free carrier concentration with increasing Tl content in the $\text{Bi}_{2-x}\text{Tl}_x\text{Se}_3$ samples, following from the above interpretation of the reflectance spectra, should result also in the decrease in the value of absorption coefficient K with increasing Tl content. This effect is evident in Fig. 4. The value of K_{\min} in the minimum of the dependence $K = f(h\nu)$ is equal to 913 cm^{-1} for pure Bi_2Se_3 ,

whereas $K_{min} = 621 \text{ cm}^{-1}$ for the $\text{Bi}_{1.9}\text{Tl}_{0.1}\text{Se}_3$ (see also Table I).

It is further evident from Fig. 4 that the presence of thallium impurities results also in a shift of the short-wavelength absorption edge towards lower energies. This implies that the incorporation of Tl atoms into the Bi_2Se_3 lattice leads to a decrease in the optical gap E_g^{opt} . Also this fact is in a good agreement with the conclusion that the thallium impurity in the Bi_2Se_3 lattice decreases the concentration of the free charge carriers. In accordance with the Moss–Burstein effect, i.e. with the shift of the short-wavelength absorption edge resulting from the change of the free carrier concentration N , with decreasing N we expect a shift of the edge towards lower energies, hence a decrease in the values of E_g^{opt} .

By the extrapolation of the short wavelength edge (K^2 vs. photon energy) to the $K = 0$ for pure Bi_2Se_3 one gets the value of the energy gap $E_g^{opt} \sim 0.24 \text{ eV}$ (not shown here). This value is in good accordance with previously published data [9].

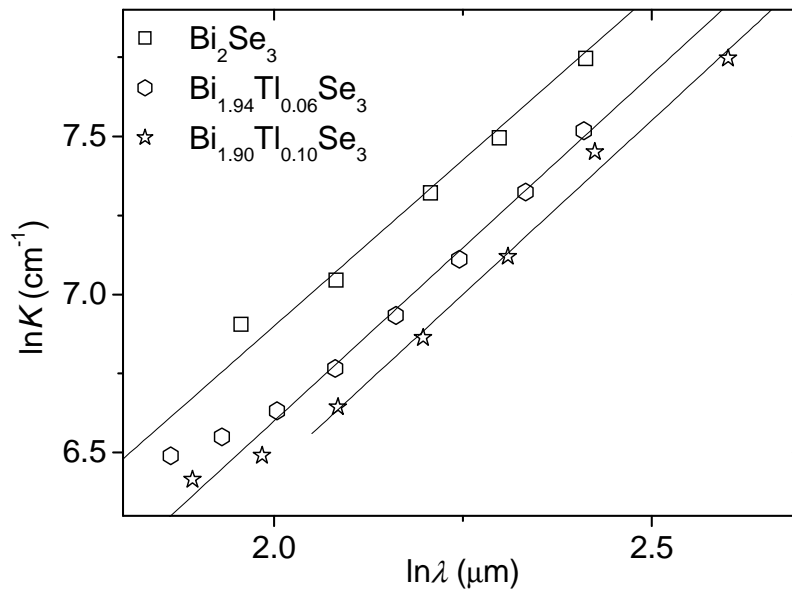


Fig. 5 Plots of $\ln K$ vs. $\ln \lambda$ for $\text{Bi}_{2-x}\text{Tl}_x\text{Se}_3$ single crystals

It is known that the shape of the long-wavelength edge gives information on the scattering mechanism of the free charge carriers. With the objective to determine the values of the exponent β in the relation $K \sim \lambda^\beta$ we have plotted the curves $\ln K$ vs. $\ln \lambda$ in Fig. 5. The values of β obtained from these plots range from 2.1 to 2.5. This indicates that in $\text{Bi}_{2-x}\text{Tl}_x\text{Se}_3$ single crystals at temperatures close to 300 K the dominant scattering mechanism of the free carriers is the scattering by the acoustic branches of lattice vibrations. The fact that the obtained values of β are higher than $3/2$, which in covalent crystals correspond to the scattering by acoustic phonons [10], can be explained assuming that in our mixed crystals we deal with a mixed scattering mechanism by acoustic phonons and ionized impurities. This view is in full agreement with the conclusion of the paper by

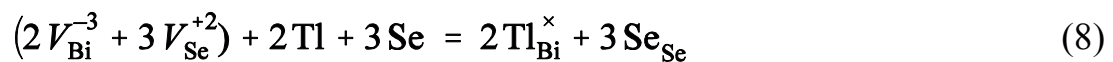
Stordeur *et al.* [11] i.e. that at room temperature the crystal lattice of Bi₂Se₃ based materials is characterized by the mixed anisotropic scattering mechanism of the free carriers by acoustic phonons and ionized impurities.

Point Defects in Bi_{2-x}Tl_xSe₃ Single Crystals

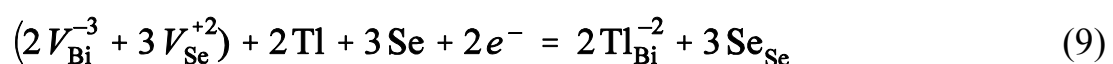
As mentioned above, doping with thallium leads to the decrease of the free electron concentration in Bi_{2-x}Tl_xSe₃ single crystals. In this paragraph we will qualitatively discuss the findings. Our consideration is based on the following points. The single crystal of Bi₂Se₃ prepared from stoichiometric melt shows an excess of bismuth over the stoichiometric composition [12]. According to the ideas presented in [13], this is the reason why the crystal lattice contains negatively charged antisite (AS) defects **Bi_{Se}⁻¹** of bismuth atoms on selenium sites and positively charged vacancies **V_{Se}⁺²** in the selenium sublattice. The concentration of vacancies [**V_{Se}⁺²**] exceeds the concentration of AS defects [**Bi_{Se}⁻¹**] and the Bi_{2+δ}Se₃ crystals exhibit n-type conductivity, the concentration of free electrons [**e⁻**] is given by the difference of the concentration of both native defects, i.e.

$$[e^-] = 2[V_{Se}^{+2}] - [Bi_{Se}^{-1}] \quad (7)$$

The results of XRD analysis presented in [6] reveal that the volume of the unit cell decreases monotonously with the increasing thallium content. We assume that thallium atoms enter the sublattice of bismuth forming Tl_{Bi} substitutional defects. Since indium is presented in valence state +3 in Bi₂Se₃ [5], we assume initially, by analogy, that thallium is also present in this valence state, i.e. it forms uncharged defects Tl_{Bi}^x



(**V_{Bi}⁻³** and **Se_{Se}** stand for bismuth vacancy and selenium atom on ordinary site). It is evident that this way thallium produces no free carriers. However thallium in state +3 can be easily reduced to valence +1 which is more stable form of thallium from the chemical point of view, i.e. it can capture two electrons from conduction band and reduce the free electron concentration



The comparison of the actual and nominal concentration of thallium in the samples gives another potential explanation of the change of the free carrier

concentration. The actual concentration of thallium is smaller by two orders of magnitude than the nominal one (see Table I). Actually we deal with doped crystals not solid solutions as perhaps suggested by the notation of the nominal composition. Only a small percentage of thallium was incorporated into the host structure, the rest was segregated on the top of the single crystal in the form of a polycrystalline lump [6]. The X-ray diffraction revealed two structures in the lump, Bi_2Se_3 and TlBiSe_2 [6]. The stoichiometry of the later implies that the single crystals grew from a nonstoichiometric melt, namely from the melt that show excess of selenium over the stoichiometric composition. Such growth conditions lead to a crystal with suppressed concentration of selenium vacancies V_{Se}^{+2} . According to equation (7) this fact can account for the observed decrease in the free electron concentration.

We note that both the formation of func $\text{TI}_{\text{Bi}}^{-2}$ and the descending vacancies V_{Se}^{+2} concentration can account for the decrease of the free electron concentration. The experimental results do not allow us to specify the dominant mechanism. However, in the view of a noticeable increase in free carrier mobility [6] we believe that the suppression of selenium vacancies is significant. A suppression rather than increase in the defect concentration is consistent with the increase in the free carrier mobility.

Conclusion

The single crystals of $\text{Bi}_{2-x}\text{Tl}_x\text{Se}_3$ ($c_{\text{Tl}} = 0.52 \times 10^{24}$ atoms m^{-3}) were prepared using the Bridgman technique. The optical properties were measured at room temperature. The results obtained from the measurement of reflectance in the plasma resonance frequency region and transmittance in the IR region of $\text{Bi}_{2-x}\text{Tl}_x\text{Se}_3$ single crystals lead to following conclusions:

1. Substitution of Bi atoms by Tl atoms in the Bi_2Se_3 crystal structure results in a decrease in the concentration of the free electrons.
2. The suppression of the free electron concentration can be ascribed to the point defects $\text{TI}_{\text{Bi}}^{-2}$ — type and to a decrease of concentration of selenium vacancies V_{Se}^{+2} .
3. The shift of the short-wavelength absorption edge to the lower energies, i.e. decrease in the optical gap E_g^{opt} as well as decrease in the absolute value of the absorption coefficient K with increasing Tl content confirm the decrease in the concentration of free electrons.
4. Mixed anisotropic scattering mechanism of the free carriers by acoustic phonons and ionized impurities was determined from the shape of long-wavelength absorption edge.

Acknowledgements

The research was supported by the Ministry of Education, Youth and Sports of the Czech Republic under project No. MSM 0021627501.

References

- [1] Nolas G.S., Sharp J., Goldsmid H.J.: *Thermoelectrics, Basic Principles and New Materials Developments*, p. 123, Springer, Berlin, 2001.
- [2] Krost A.: in Landolt-Börnstein (New Series), Group III, Vol. 17f, p. 268, Berlin/Heidelberg, New York/Tokyo, 1989.
- [3] Horák J., Lošťák P., Montaner A.: *Phys. Stat. Sol. (b)* **119**, K17 (1983).
- [4] Lošťák P., Novotný R., Urbanová E., Horák J.: *Phys. Stat. Sol. (a)* **113**, 615 (1989).
- [5] Lošťák P., Beneš L., Civiš S., Süßmann H.: *J. Mater. Sci.* **25**, 277 (1990).
- [6] Janíček P., Drašar Č., Beneš L., Lošťák P.: *Cryst. Res. Technol.* **44**, 505 (2009).
- [7] Madelung O.: *Handbuch der Physik*, Vol. 20, (Ed. S. Flügge) p. 210, Springer, Berlin, 1957.
- [8] Kulbachinskii V.A., Miura N., Nakagawa H., Arimoto H., Ikaida T., Lošťák P., Drašar Č.: *Phys. Rev. B* **59**, 15733 (1999).
- [9] Hashimoto K., *Fyc. Sci-Kyushu Univ. B* **2**, 141 (1958).
- [10] Yakovlev A.: *Fiz. Tverd. Tela* **2**, 1621 (1960).
- [11] Stordeur M., Ketavong K.K., Priemuth A., Sobotta H., Riede V.: *Phys. Stat. Sol. (b)* **169**, 505 (1992).
- [12] Offergeld G., Cakenberghe J.: *J. Phys. Chem. Solids* **11**, 301 (1959).
- [13] Sklenář A., Drašar Č., Krejčová A., A., Lošťák P.: *Crys. Res. Technol.* **35**, 1069 (2000).